Study of TileCal performance using 2015 and 2023 cosmic-ray data

Archil Durglishvili (HEPI TSU), Claudio Santoni (LPC Clermont Ferrand)

03/10/2024

TileCal Calibration, Data Preparation and Performance in Tile Week

Introduction

Cosmic-ray muons can be used to study:

a) cell response uniformity in η and φ

b) stability of the response in different data periods

c) layers inter-calibration

d) layer energy measurement scale

Combination of 2008-2023 cosmic-ray data to study the **layer response stability, uniformity and energy scale** is documented in the note: ATL-COM-TILECAL-2024-003

The note is under review process (referees: Tomas and Giulio)

The study uses:

- 2008-2010 cosmic-ray data from the PUB note
- 2015 and 2023 data from the ongoing analysis that is being documented
- **Run1 cosmic-ray MC** results from the PUB note

The analysis of cosmic-ray data 2015 and 2023 is being documented

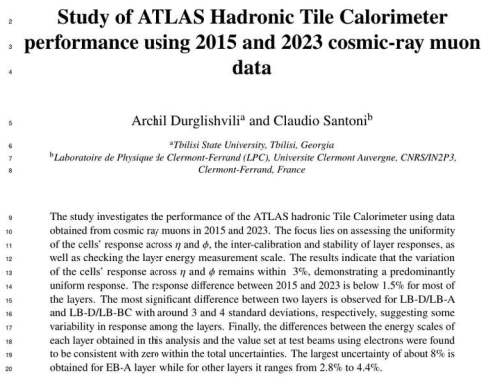

Study of ATLAS Hadronic Tile Calorimeter performance using 2015 and 2023 cosmic-ray muon data

Archil Durglishvili[a] and Claudio Santoni[b]

[a]*Tbilisi State University, Tbilisi, Georgia*
[b]*Laboratoire de Physique de Clermont-Ferrand (LPC), Universite Clermont Auvergne, CNRS/IN2P3, Clermont-Ferrand, France*

The study investigates the performance of the ATLAS hadronic Tile Calorimeter using data obtained from cosmic ray muons in 2015 and 2023. The focus lies on assessing the uniformity of the cells' response across η and ϕ, the inter-calibration and stability of layer responses, as well as checking the layer energy measurement scale. The results indicate that the variation of the cells' response across η and ϕ remains within 3%, demonstrating a predominantly uniform response. The response difference between 2015 and 2023 is below 1.5% for most of the layers. The most significant difference between two layers is observed for LB-D/LB-A and LB-D/LB-BC with around 3 and 4 standard deviations, respectively, suggesting some variability in response among the layers. Finally, the differences between the energy scales of each layer obtained in this analysis and the value set at test beams using electrons were found to be consistent with zero within the total uncertainties. The largest uncertainty of about 8% is obtained for EB-A layer while for other layers it ranges from 2.8% to 4.4%.

The study uses:

- 2015 cosmic runs with both magnets ON
- 2023 cosmic runs with both magnets ON
- **Run3 simulation of single muon events**

The analysis is ongoing and only preliminary results are presented

Data samples

Cosmic-ray muon data of 2015 and 2023

runs with magnets ON

physics_IDCosmic stream

The runs are reconstructed with the latest calibration constants

Many thanks to Siarhei and Sasha

TCAL1 derivations

2015 datasets
data15_cos.00271967.physics_IDCosmic.merge.RAW
data15_cos.00271965.physics_IDCosmic.merge.RAW
data15_cos.00271958.physics_IDCosmic.merge.RAW
data15_cos.00271957.physics_IDCosmic.merge.RAW
data15_cos.00271916.physics_IDCosmic.merge.RAW
data15_cos.00271859.physics_IDCosmic.merge.RAW
data15_cos.00271221.physics_IDCosmic.merge.RAW
data15_cos.00271220.physics_IDCosmic.merge.RAW
data15_cos.00271216.physics_IDCosmic.merge.RAW
data15_cos.00271199.physics_IDCosmic.merge.RAW
data15_cos.00266723.physics_IDCosmic.merge.RAW
data15_cos.00266720.physics_IDCosmic.merge.RAW
data15_cos.00266676.physics_IDCosmic.merge.RAW
data15_cos.00266667.physics_IDCosmic.merge.RAW
data15_cos.00266663.physics_IDCosmic.merge.RAW
data15_cos.00260658.physics_IDCosmic.merge.RAW
data15_cos.00260653.physics_IDCosmic.merge.RAW
data15_cos.00260650.physics_IDCosmic.merge.RAW
data15_cos.00260095.physics_IDCosmic.merge.RAW
data15_cos.00260094.physics_IDCosmic.merge.RAW
data15_cos.00259921.physics_IDCosmic.merge.RAW
data15_cos.00258865.physics_IDCosmic.merge.RAW
data15_cos.00258769.physics_IDCosmic.merge.RAW
data15_cos.00258764.physics_IDCosmic.merge.RAW
data15_cos.00258755.physics_IDCosmic.merge.RAW
data15_cos.00258750.physics_IDCosmic.merge.RAW
data15_cos.00258745.physics_IDCosmic.merge.RAW
data15_cos.00258727.physics_IDCosmic.merge.RAW
data15_cos.00258617.physics_IDCosmic.merge.RAW
data15_cos.00258544.physics_IDCosmic.merge.RAW
data15_cos.00258543.physics_IDCosmic.merge.RAW
data15_cos.00258449.physics_IDCosmic.merge.RAW
data15_cos.00258389.physics_IDCosmic.merge.RAW
data15_cos.00258356.physics_IDCosmic.merge.RAW
data15_cos.00258342.physics_IDCosmic.merge.RAW
data15_cos.00258337.physics_IDCosmic.merge.RAW
data15_cos.00258303.physics_IDCosmic.merge.RAW
data15_cos.00258274.physics_IDCosmic.merge.RAW
data15_cos.00258263.physics_IDCosmic.merge.RAW

2023 datasets
data23_cos.00453177.physics_IDCosmic.merge.RAW
data23_cos.00453220.physics_IDCosmic.merge.RAW
data23_cos.00453239.physics_IDCosmic.merge.RAW
data23_cos.00454833.physics_IDCosmic.merge.RAW
data23_cos.00454954.physics_IDCosmic.merge.RAW
data23_cos.00455088.physics_IDCosmic.merge.RAW
data23_cos.00455178.physics_IDCosmic.merge.RAW
data23_cos.00454957.physics_IDCosmic.merge.RAW
data23_cos.00457007.physics_IDCosmic.merge.RAW
data23_cos.00457076.physics_IDCosmic.merge.RAW
data23_cos.00457162.physics_IDCosmic.merge.RAW
data23_cos.00457192.physics_IDCosmic.merge.RAW
data23_cos.00457238.physics_IDCosmic.merge.RAW
data23_cos.00457413.physics_IDCosmic.merge.RAW
data23_cos.00456956.physics_IDCosmic.merge.RAW
data23_cos.00457324.physics_IDCosmic.merge.RAW
data23_cos.00457411.physics_IDCosmic.merge.RAW
data23_cos.00457412.physics_IDCosmic.merge.RAW
data23_cos.00457509.physics_IDCosmic.merge.RAW
data23_cos.00459263.physics_IDCosmic.merge.RAW
data23_cos.00459450.physics_IDCosmic.merge.RAW
data23_cos.00459686.physics_IDCosmic.merge.RAW

Run3 MC simulation

- The single muon events are simulated with the momentum, eta and phi spectra measured in cosmic-ray data 2023
- Simulation is done using Athena release 23.0.49 (Run3 setup)
- **Cell responses are corrected for the difference in the sampling fraction between Rel22 and Rel23**

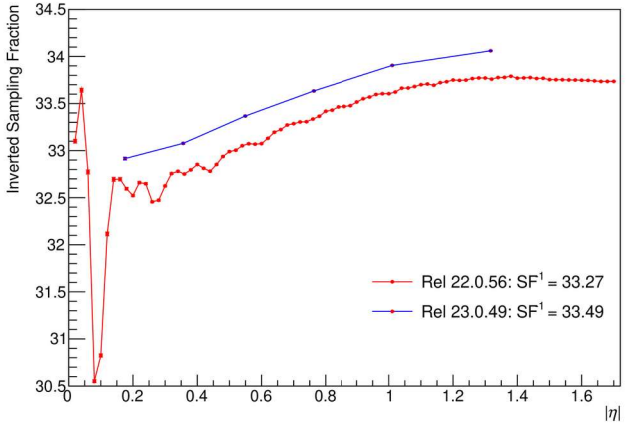

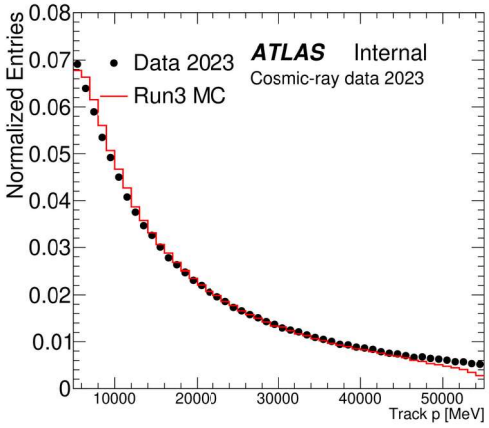

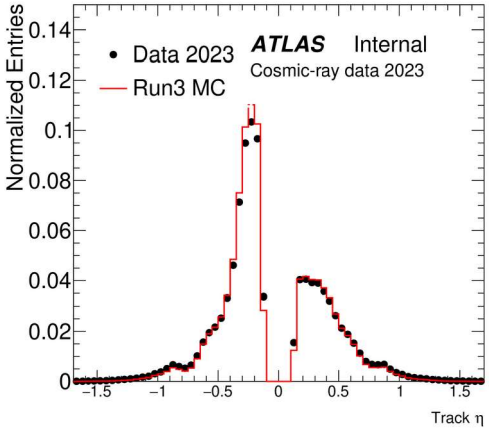

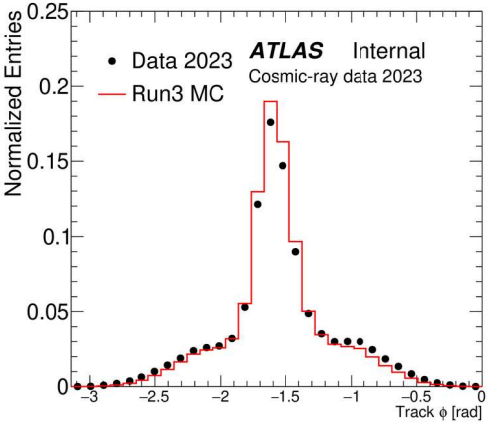

Analysis method

- The analysis uses the muon tracks reconstructed in the Inner Detector
- Tracks are extrapolated to the TileCal layers and the path length (*dl*) in the traversed cells is calculated
- The energy deposited per unit of path length (*dE/dl*) is used to study the TileCal performance
- Cosmic-ray muon tracks are reconstructed in the downstream of the inner detector, therefore, only cells in the lower part of the calorimeter were used in the analysis to have a better path reconstruction

Selection

Event selection

Exactly one *combined* muon

At least 8 pixel hits

$|d_0|$ < 380mm and $|z_0|$ < 800mm

$|\theta|$ > 0.13 rad

10 < p^{track} < 30 GeV

Selection	2015		2023	
	Yield	Fraction	Yield	Fraction
Triggered events	3812221	1.00	4071604	1.00
=1 muon	446935	0.12	840070	0.21
$N^{\text{pixel hits}} \geq 8$	444547	0.12	839871	0.21
$\lvert d_0^{\text{trk}} \rvert \leq 380\ mm$ and $\lvert z_0^{\text{trk}} \rvert \leq 800\ mm$	387857	0.10	777346	0.19
$\lvert\theta\rvert > 0.13$ rad	314947	0.08	666927	0.16
$10 \leq p \leq 30$ GeV	113715	0.03	244657	0.06

Cell selection

Path length dx > 200 mm

$|\Delta\phi$(cell,track)| < 0.04 rad

Cell energy dE > 60 MeV

Selection	MC		2015		2023	
	Yield	Fraction	Yield	Fraction	Yield	Fraction
Signals of the cells crossed by the selected tracks	1904397	1.00	441217	1.00	871005	1.00
$dl > 200$ mm	1386041	0.73	318054	0.72	626154	0.72
$\lvert\Delta\phi\rvert < 0.04$ rad	1111153	0.58	253558	0.57	499711	0.57
$dE > 60$ MeV	1107162	0.58	250710	0.57	497381	0.57

dE/dl distributions

- Example *dE/dl* distributions are shown for A3 and D2 cells
- Results from Run1 analysis are shown for comparison

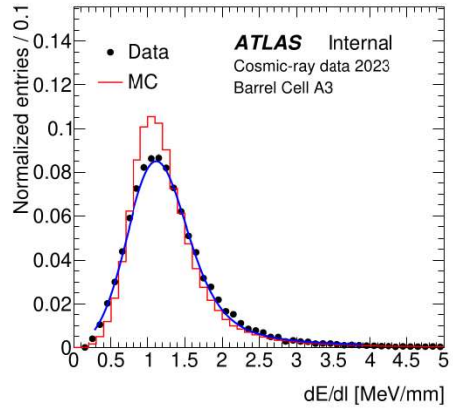

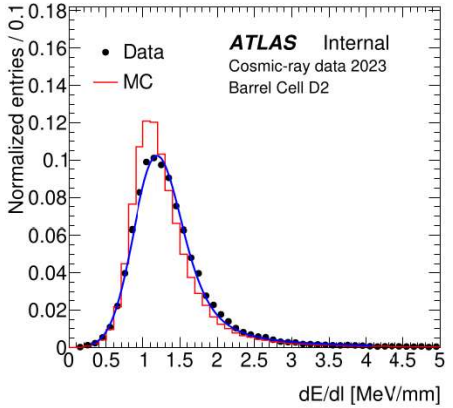

ATL-TILECAL-PUB-2011-001:

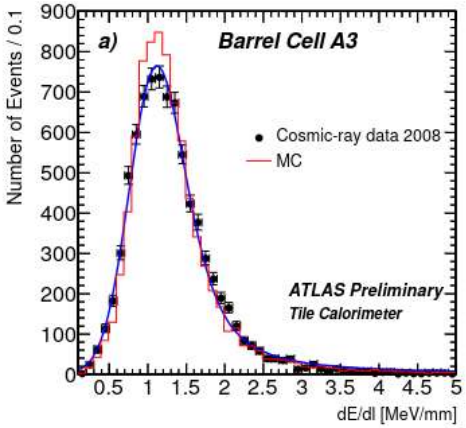

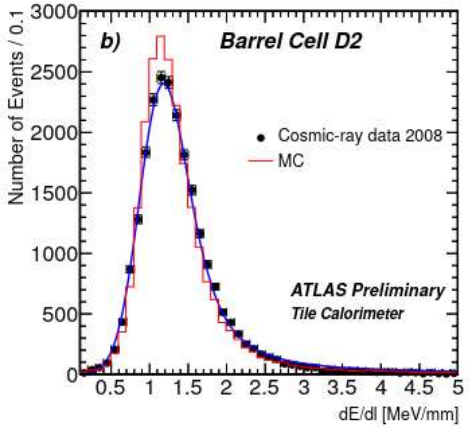

Cell response

- The cell response is defined as the truncated mean of the *dE/dl* distribution, $\langle dE/dl \rangle_T$, computed by truncating F = 1% fraction of entries in the upper side of the distribution
- The cell response uniformity is studied using data-to-MC ratio of truncated means:

$$R = \frac{\langle dE/dl \rangle_T^{\text{Data}}}{\langle dE/dl \rangle_T^{\text{MC}}}$$

- Taking the ratio of truncated means between experimental and simulated data largely compensates systematics effects

Cell response uniformity in eta (Long Barrel)

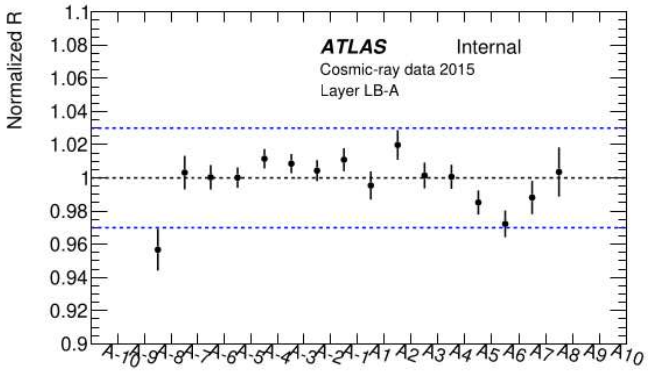

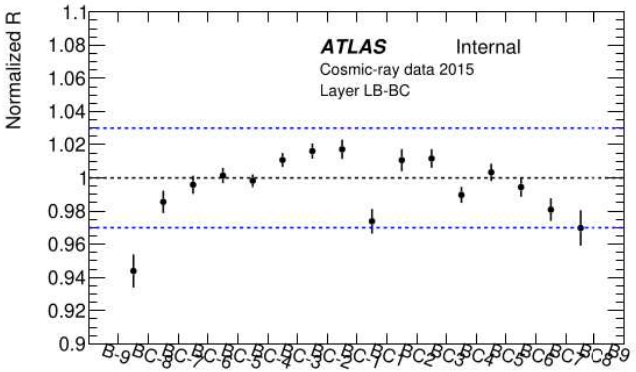

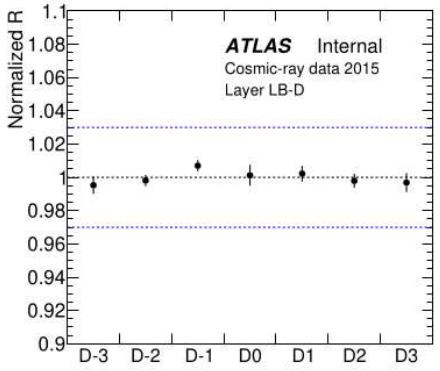

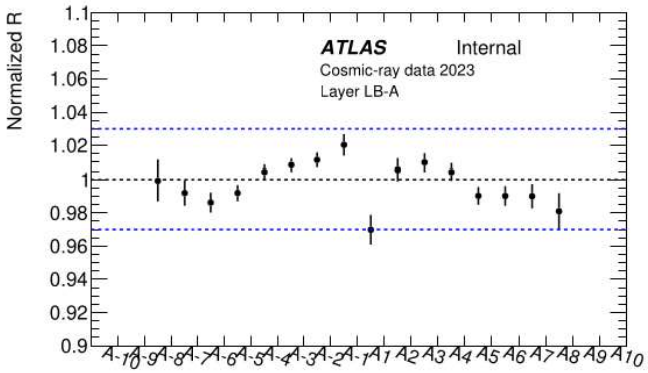

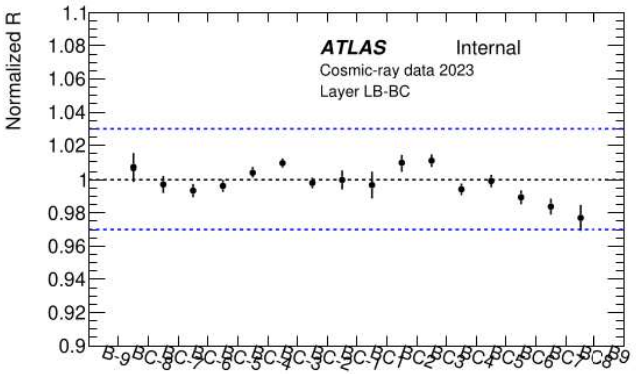

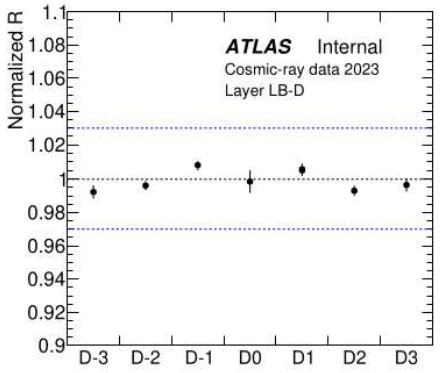

Data-to-MC ratio values as a function cell type are scattered mostly within ±2%

Cell response uniformity in eta (Extended Barrel)

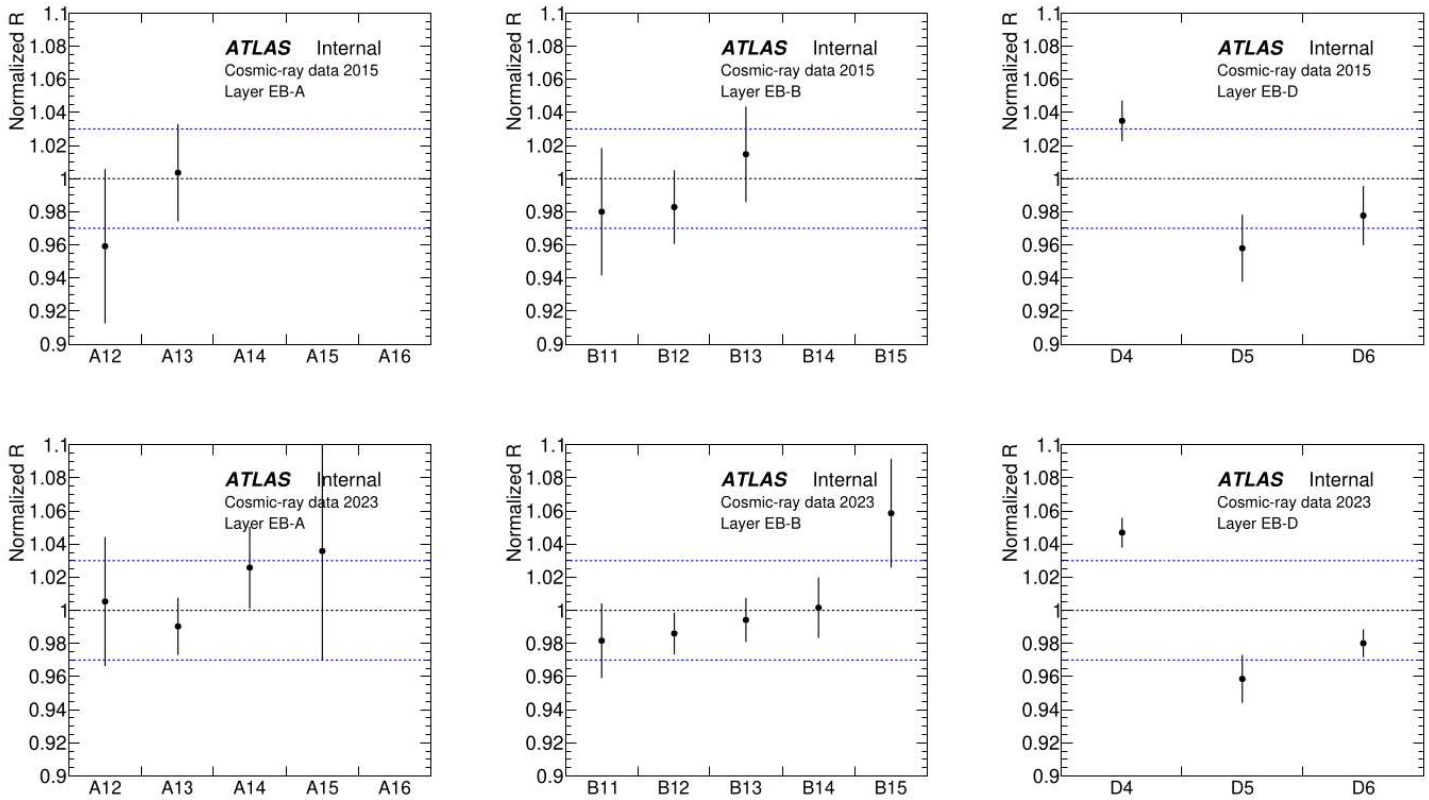

Data-to-MC ratio values as a function cell type are scattered mostly within ±3%

Cell response uniformity in phi (Long Barrel)

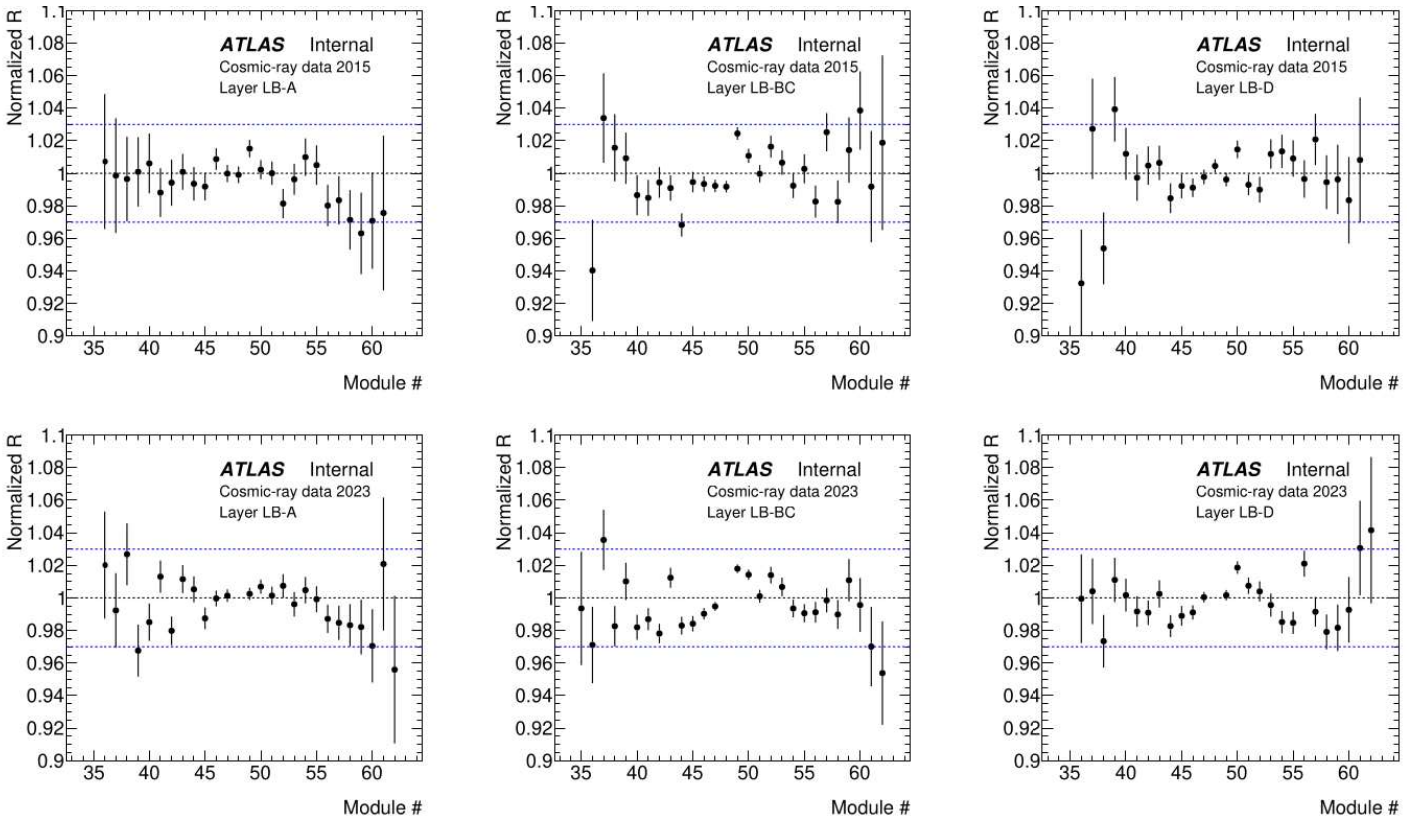

Data-to-MC ratio values as a function of module number are scattered mostly within ±3%

Cell response uniformity in phi (Extended Barrel)

In 2015 data, number of entries for EB-A and EB-B layers in individual modules is below 100, therefore, 1% truncated mean can not be calculated

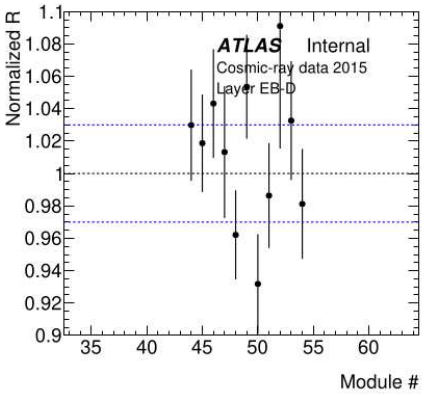

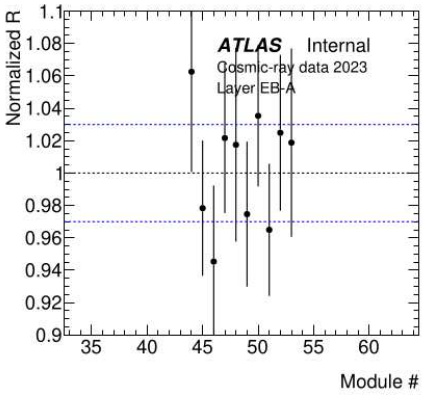

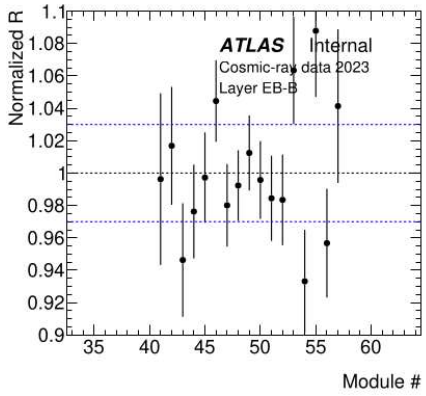

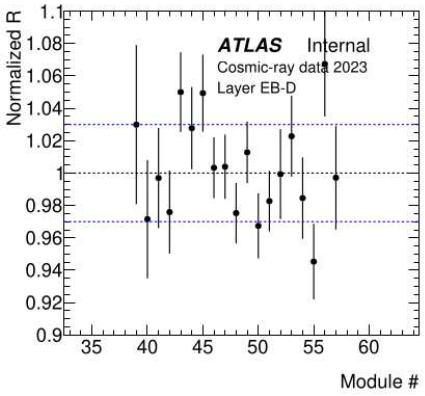

Data-to-MC ratio values as a function of module number are scattered mostly within ±3%

Layer response

- The layer response is defined as the truncated mean of a *dE/dl* distribution obtained using all selected cell signals in a given layer
- The layer response uniformity and scale are studied using data-to-MC ratio of layer responses:

$$R^{l} = \frac{\langle dE/dl \rangle_{\mathrm{T}}^{l,\mathrm{Data}}}{\langle dE/dl \rangle_{\mathrm{T}}^{l,\mathrm{MC}}}$$

- Taking the ratio of truncated means between experimental and simulated data largely compensates systematics effects

Layer response determinations

Layer	$\langle dE/dl \rangle_T^l$ [MeV/mm]		
	MC	Data 2015	Data 2023
LB-A	1.2834 ± 0.0010	1.2824 ± 0.0022	1.2984 ± 0.0016
LB-BC	1.3179 ± 0.0007	1.3394 ± 0.0017	1.3462 ± 0.0011
LB-D	1.3026 ± 0.0009	1.3618 ± 0.0020	1.3718 ± 0.0014
EB-A	1.314 ± 0.011	1.242 ± 0.025	1.325 ± 0.013
EB-B	1.323 ± 0.005	1.327 ± 0.019	1.310 ± 0.007
EB-D	1.313 ± 0.004	1.323 ± 0.011	1.342 ± 0.006

Only statistical uncertainties are presented.

The largest difference between the responses of two layers is about 10% (6%) in data 2015 (data 2023).
To establish the significance of the differences, both statistical and systematic uncertainties has to be taken into account.

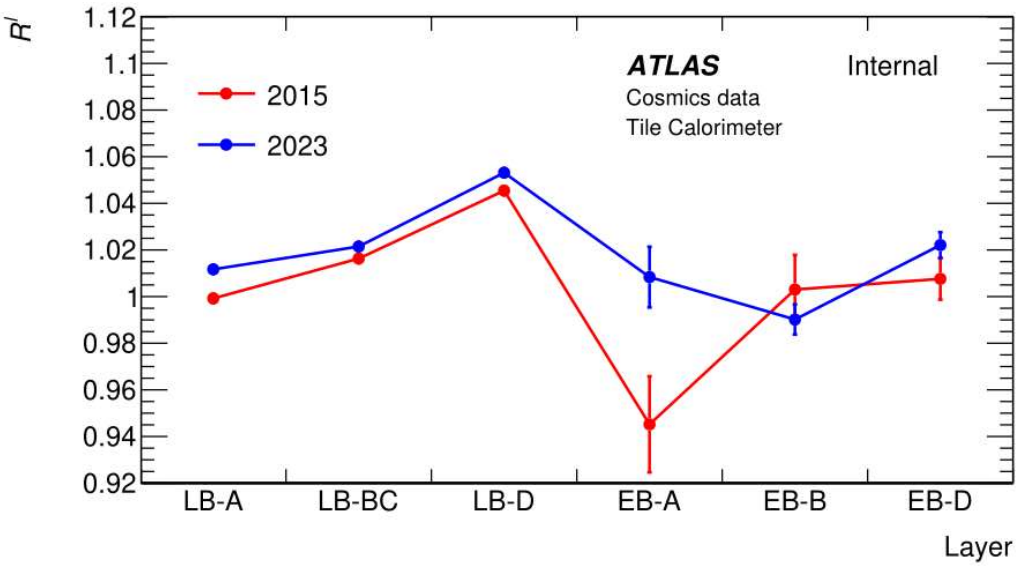

Layer response stability

The stability is checked by comparing individual layer response between 2015 and 2023 data

Layer:	LB-A	LB-BC	LB-D	EB-A	EB-B	EB-D
$\frac{\langle dE/dl \rangle_{\mathrm{T}}^{l,2023}}{\langle dE/dl \rangle_{\mathrm{T}}^{l,2015}}$:	1.0125 ± 0.0021	1.0051 ± 0.0015	1.0073 ± 0.0018	1.067 ± 0.024	0.987 ± 0.015	1.014 ± 0.010

Only statistical uncertainties are presented.
Since the stability check involves comparing responses of the same layer, systematic uncertainties cancel.

The largest difference of 6.7% is observed for EB-A layer, however, the statistical significance of the difference is below 3σ.
The response difference for all other layers is below 1.5%, with the uncertainty better than 1.5%.

Layer response uniformity (inter-calibration)

- The agreement between each pair of layer responses is evaluated as:

$$\Delta^{l,l'} = 1 - R^{l,l'}$$

where

$$R^{l,l'} \equiv \frac{R^{l}}{R^{l'}}$$

- Systematic uncertainties are determined on $R^{l,l'}$ to establish the significance of the disagreement between two layer responses

Systematic uncertainties on $R^{l,l'}$

Uncertainty source		$R^{2,1}$	$R^{3,1}$	$R^{4,1}$	$R^{5,1}$	$R^{6,1}$	$R^{3,2}$	$R^{4,2}$	$R^{5,2}$	$R^{6,2}$	$R^{4,3}$	$R^{5,3}$	$R^{6,3}$	$R^{5,4}$	$R^{6,4}$	$R^{6,5}$
Statistics		0.17	0.19	1.28	0.70	0.55	0.16	1.28	0.69	0.55	1.28	0.70	0.55	1.45	1.38	0.87
S_1	$\lvert\theta\rvert > 0.10$ rad	0.44	0.54	0.51	0.51	0.51	0.1	0.07	0.07	0.07	0.03	0.03	0.03	0.0	0.0	0.0
	$\lvert\theta\rvert > 0.15$ rad	0.05	0.0	0.1	0.1	0.1	0.04	0.06	0.06	0.06	0.1	0.1	0.1	0.0	0.0	0.0
S_2	$30 < p < 50$ GeV	0.3 ± 0.4	0.2 ± 0.4	7.4 ± 2.4	1.9 ± 1.4	0.3 ± 1.1	0.11 ± 0.35	7.7 ± 2.4	1.6 ± 1.3	0.6 ± 1.0	7.6 ± 2.4	1.7 ± 1.3	0.5 ± 1.1	10.1 ± 3.2	7.7 ± 3.0	2.2 ± 1.6
	$5 < p < 10$ GeV	0.41 ± 0.27	0.75 ± 0.28	5.3 ± 3.0	1.7 ± 1.6	1.1 ± 1.2	0.35 ± 0.25	4.9 ± 3.0	1.3 ± 1.6	1.5 ± 1.2	4.5 ± 3.0	1.0 ± 1.7	1.8 ± 1.2	4 ± 4	7 ± 4	2.8 ± 2.1
S_3	$dl > 150$ mm	0.18	0.23	0.23	0.07	0.01	0.05	0.05	0.11	0.17	0.0	0.16	0.22	0.15	0.22	0.06
	$dl_c > dl_c^{min}$	0.43	0.41	0.56	0.4	0.17	0.03	0.13	0.03	0.6	0.15	0.01	0.58	0.16	0.73	0.57
	$200 < dl_c < dl_c^{max}$	0.22	0.26	0.77	0.61	1.79	0.03	0.55	0.38	2.02	0.51	0.35	2.05	0.17	2.58	2.41
S_4	$\lvert\Delta\phi\rvert < 0.03$ rad	0.33	0.12	0.51	0.58	0.39	0.21	0.18	0.26	0.71	0.39	0.47	0.5	0.07	0.9	0.97
	$\lvert\Delta\phi\rvert < 0.05$ rad	0.18	0.48	0.26	0.0	0.43	0.3	0.44	0.18	0.25	0.75	0.48	0.05	0.26	0.69	0.43
S_5	$dE > 0$ MeV	0.32	0.36	0.33	0.12	3.69	0.04	0.65	0.2	3.36	0.69	0.24	3.32	0.45	4.03	3.57
	$E^{\mathrm{PMT}} > 60$ MeV	1.29	1.16	1.49	1.06	0.34	0.12	0.2	0.23	0.94	0.32	0.11	0.82	0.42	1.13	0.71
S_6	$F = 2\%$	0.08	0.0	0.34	0.19	0.08	0.08	0.42	0.11	0.16	0.34	0.19	0.08	0.53	0.26	0.27
	$F = 0\%$	0.02	0.02	1.08	0.96	0.12	0.04	1.1	0.94	0.1	1.06	0.98	0.13	2.01	1.18	0.85
S_7	Data vs MC difference in the spread of dE/dl distributions	0.4	0.4	0.4	0.4	0.4	0.4	0.4	0.4	0.4	0.4	0.4	0.4	0.4	0.4	0.4
S_8	Radial calibration correction	0.4	0.4	0.4	0.4	0.4	0.4	0.4	0.4	0.4	0.4	0.4	0.4	0.4	0.4	0.4
S_9	Up-drift and magnetic field effects	0.0	0.0	0.4	0.4	0.4	0.0	0.4	0.4	0.4	0.4	0.4	0.4	0.0	0.0	0.0
S_{10}	MC SF angle-dependence	0.02	0.13	2.99	2.86	2.36	0.11	3.0	2.87	2.38	3.12	2.99	2.49	0.13	0.61	0.48
Total systematics		1.58	1.55	8.17	3.27	4.78	0.68	8.26	3.11	4.7	8.22	3.22	4.68	10.29	4.86	4.48

Effects of individual uncertainty sources are shown in percentage.

Maximum effect of each source of systematic uncertainty, that is above the statistical uncertainty, is added in quadrature to calculate the total systematic uncertainty.

Determinations of $\Delta^{l,l'}$ (in percentage)

Using data 2015

l/l'	LB-A	LB-BC	LB-D	EB-A	EB-B	EB-D
LB-A		-1.7 ± 1.6	-4.6 ± 1.6	5 ± 8	-0 ± 4	-1 ± 5
LB-BC			-2.9 ± 0.7	7 ± 8	1.3 ± 3.4	1 ± 5
LB-D				10 ± 8	4.1 ± 3.4	4 ± 5
EB-A					-6 ± 11	-7 ± 6
EB-B						-0 ± 5
EB-D						

Using data 2023

l/l'	LB-A	LB-BC	LB-D	EB-A	EB-B	EB-D
LB-A		-1.0 ± 1.6	-4.1 ± 1.6	0 ± 8	2.1 ± 3.3	-1 ± 5
LB-BC			-3.1 ± 0.7	1 ± 8	3.1 ± 3.1	-0 ± 5
LB-D				4 ± 8	6.0 ± 3.1	3 ± 5
EB-A					2 ± 10	-1 ± 5
EB-B						-3 ± 5
EB-D						

- The statistical and systematic uncertainties are added in quadrature
- In both data periods, the most significant difference between two layers is observed for LB-D/LB-A and LB-D/LB-BC with around 3σ and 4σ, respectively.

Layer energy measurement scale check

- The difference between the data-to-MC ratio of the layer response and the unit

$$\delta^{l}_{EM} = R^{l} - 1$$

  is attributed to a difference between the cell energy measurement scale currently used in ATLAS and the one that is fixed at Test Beams.
- Systematic uncertainties are determined on R^{l}, and are strongly correlated between layers.

Systematic uncertainties on R^l

	Uncertainty source	$R^{\text{LB-A}}$	$R^{\text{LB-BC}}$	$R^{\text{LB-D}}$	$R^{\text{EB-A}}$	$R^{\text{EB-B}}$	$R^{\text{EB-D}}$
	Statistics	0.14	0.1	0.12	1.27	0.69	0.54
S_1	$\lvert\theta\rvert > 0.10$ rad	0.51	0.07	0.03	0.0	0.0	0.0
	$\lvert\theta\rvert > 0.15$ rad	0.1	0.06	0.1	0.0	0.0	0.0
S_2	$30 < p < 50$ GeV	0.28 ± 0.31	0.03 ± 0.22	0.12 ± 0.27	7.7 ± 2.4	1.6 ± 1.3	0.6 ± 1.0
	$5 < p < 10$ GeV	0.37 ± 0.22	0.06 ± 0.16	0.40 ± 0.19	4.9 ± 3.0	1.4 ± 1.6	1.4 ± 1.2
S_3	$dl > 150$ mm	0.25	0.07	0.02	0.03	0.18	0.24
	$dl_c > dl_c^{min}$	0.44	0.01	0.04	0.11	0.05	0.61
	$200 < dl_c < dl_c^{max}$	0.3	0.08	0.04	0.47	0.31	2.1
S_4	$\lvert\Delta\phi\rvert < 0.03$ rad	0.3	0.03	0.18	0.21	0.27	0.69
	$\lvert\Delta\phi\rvert < 0.05$ rad	0.09	0.09	0.39	0.35	0.09	0.34
S_5	$dE > 0$ MeV	0.38	0.06	0.02	0.71	0.26	3.29
	$E^{\text{PMT}} > 60$ MeV	1.98	0.72	0.84	0.52	0.94	1.65
S_6	$F = 2\%$	0.0	0.07	0.0	0.34	0.19	0.08
	$F = 0\%$	0.13	0.16	0.12	0.94	1.1	0.25
S_7	Data vs MC difference in the spread of dE/dl distributions	0.3	0.3	0.3	0.3	0.3	0.3
S_8	Radial calibration correction	0.3	0.3	0.3	0.3	0.3	0.3
S_9	Up-drift and magnetic field effects	1.0	1.0	1.0	0.6	0.6	0.6
S_{10}	MC SF angle-dependence	0.	0.	0.	0.	0.	0.
S_{11}	The simulation of the muon and electron calorimeter response	1.3	1.3	1.3	1.3	1.3	1.3
S_{12}	The determination of the EM scale at the Test Beams	0.5	0.5	0.5	0.5	0.5	0.5
	Total systematics	2.76	1.91	1.99	7.84	2.14	4.27

Effects of individual uncertainty sources are shown in percentage.

Maximum effect of each source of systematic uncertainty, that is above the statistical uncertainty, is added in quadrature to calculate the total systematic uncertainty.

Layer energy measurement scale check

Using data 2015

Layer	δ^{l}_{EM}	Stat.	Syst.	Tot.
LB-A	-0.08	± 0.19	± 2.76	± 2.77
LB-BC	1.63	± 0.14	± 1.91	± 1.91
LB-D	4.54	± 0.17	± 1.99	± 2.0
EB-A	-5.5	± 2.1	± 7.84	± 8.14
EB-B	0.3	± 1.5	± 2.14	± 2.6
EB-D	0.8	± 0.9	± 4.27	± 4.36

Using data 2023

Layer	δ^{l}_{EM}	Stat.	Syst.	Tot.
LB-A	1.17	± 0.15	± 2.76	± 2.76
LB-BC	2.15	± 0.10	± 1.91	± 1.91
LB-D	5.31	± 0.13	± 1.99	± 1.99
EB-A	0.8	± 1.3	± 7.84	± 7.95
EB-B	-1.0	± 0.6	± 2.14	± 2.24
EB-D	2.2	± 0.6	± 4.27	± 4.3

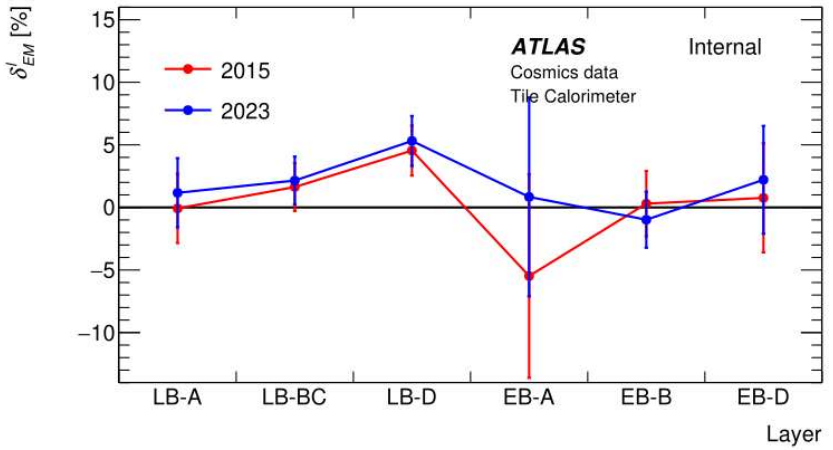

- Systematic uncertainties are strongly correlated between the layers
- The most significant deviation from zero is observed for LB-D layer of 4.5% (5.3%) with the significance of 2.3 (2.7) standard deviation in data 2015 (2023).
- The absolute difference for other layers ranges from 0.1% to 5.5%. The largest uncertainty of about 8% is obtained for EB-A layer, while for other layers it ranges from 2.8% to 4.4%.

Summary

Preliminary results of cosmic-ray data 2015 and 2023 analysis is presented

- The variation of the cells' response across η and ϕ remains within 3%, demonstrating a predominantly uniform response.
- The largest difference of 6.7% between 2015 and 2023 observed for EB-A layer has the statistical significance below 3 sigma, while for other layers the difference is below 1.5%, with the uncertainty better than 1.5%.
- The most significant difference between two layer responses is observed for LB-D/LB-A and LB-D/LB-BC with around 3 and 4 standard deviations, respectively, suggesting some variability in response among the layers.
- The most significant difference between the energy measurement scale in ATLAS and the one expected from TB is observed for LB-D layer of 4.5% (5.3%) with the significance of 2.3 (2.7) standard deviation in data 2015 (2023). For other layers the difference is compatible with zero within the uncertainties. The largest uncertainty of about 8% is obtained for EB-A layer, while for other layers it ranges from 2.8% to 4.4%.

Thanks for your attention

Backup

Longitudinal and transverse track impact parameters

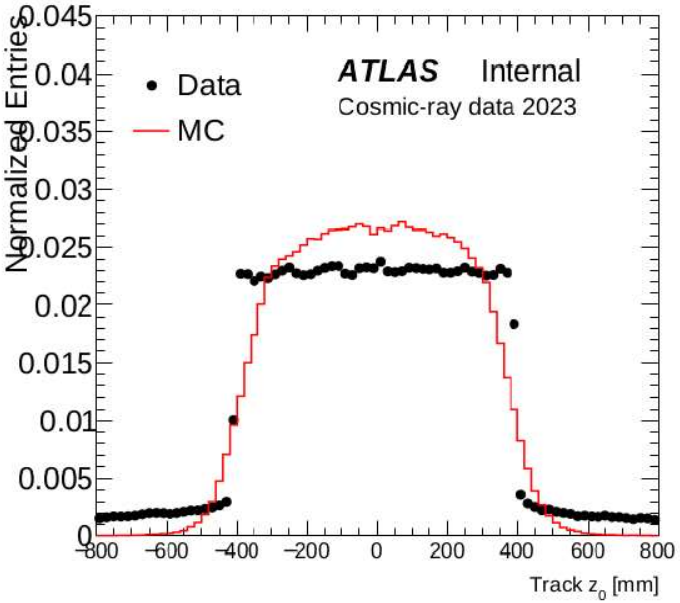

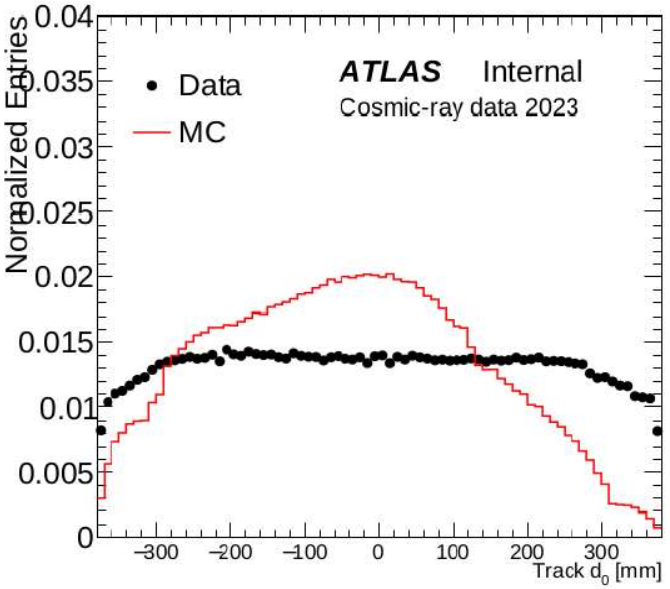

There is some difference between data and MC in the d0/z0 distributions, however, TileCal response does not depend on these variables (see next slides)

Truncated mean vs d_0/z_0

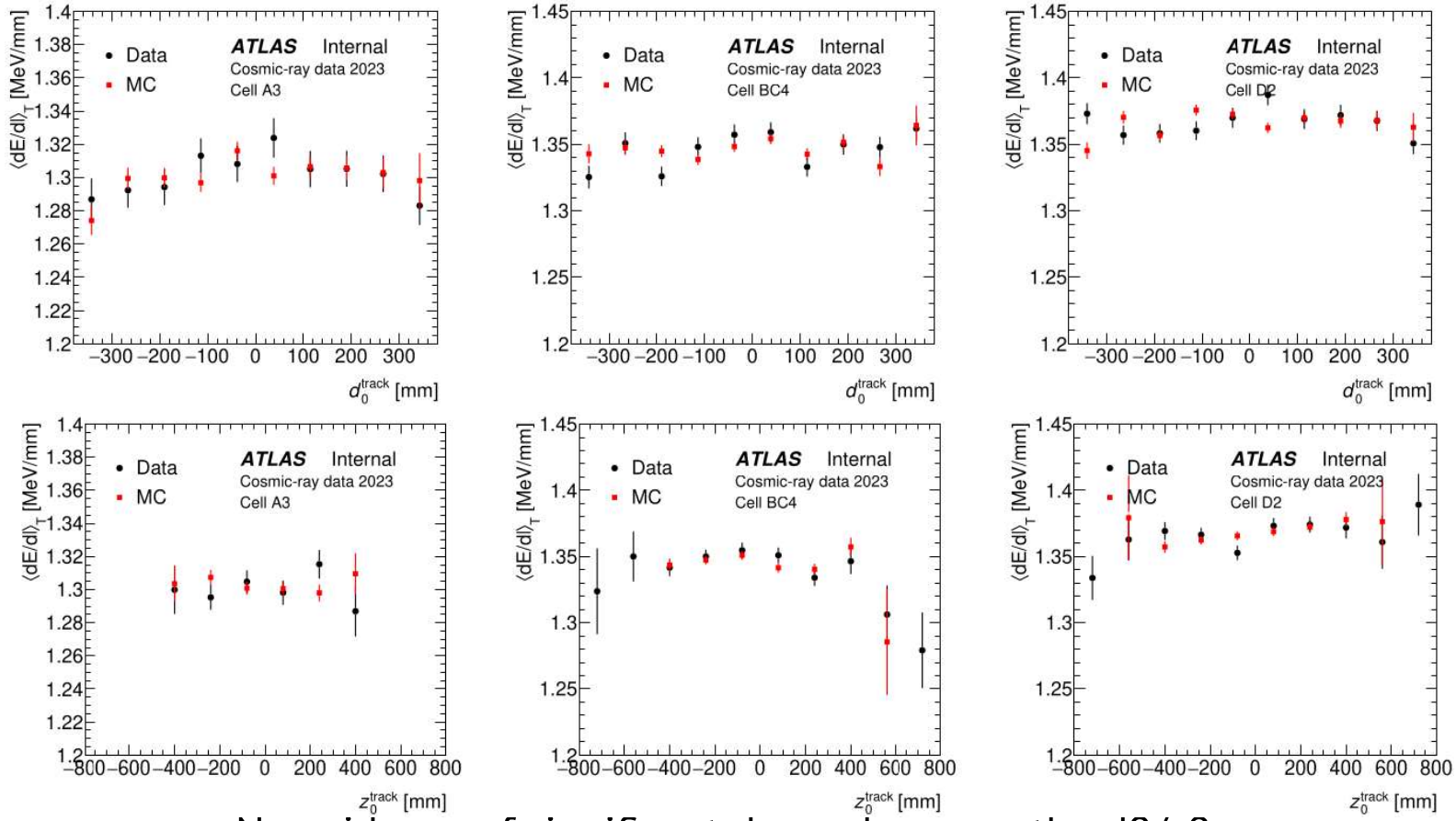

No evidence of significant dependence on the d0/z0

Impact of d0/z0 distributions on the layer response

Layer	Pseudo-projective muons MC	Projective muons MC	Ratio
LB-A	1.2834+/-0.0010	1.2879+/-0.0007	1.0035+/-0.0010
LB-BC	1.3179+/-0.0007	1.3202+/-0.0005	1.0017+/-0.0007
LB-D	1.3026+/-0.0009	1.3059+/-0.0007	1.0025+/-0.0009
EB-A	1.314+/-0.011	1.306+/-0.006	0.994+/-0.009
EB-B	1.323+/-0.005	1.3305+/-0.0033	1.006+/-0.005
EB-D	1.313+/-0.004	1.3192+/-0.0025	1.005+/-0.004

Impact of d0/z0 distributions on the layer response is negligible

Response dependence on the path length

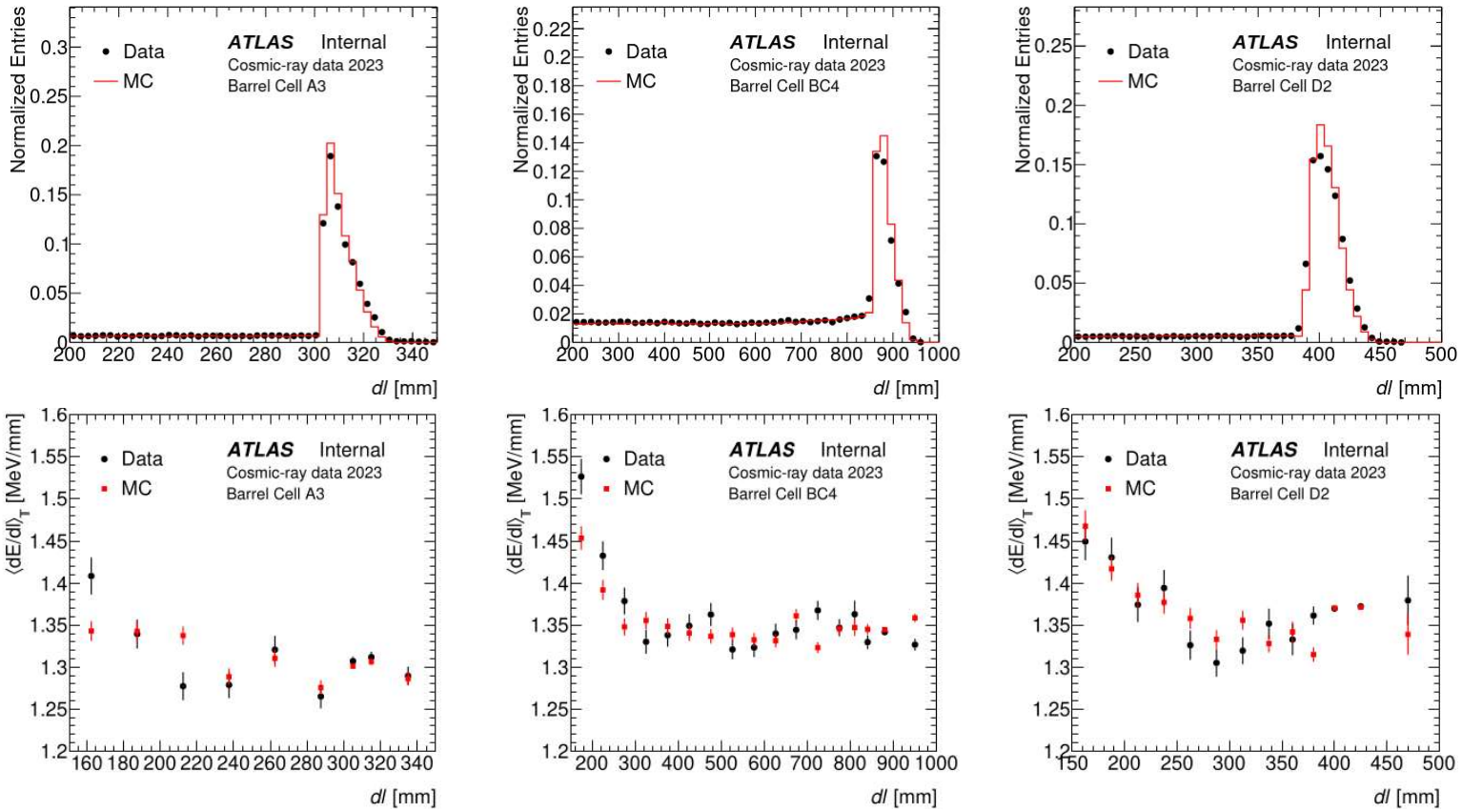

The MC well reproduces the path length distributions and the response dependence on path length observed in the data

Data/MC of average path length as a function of eta

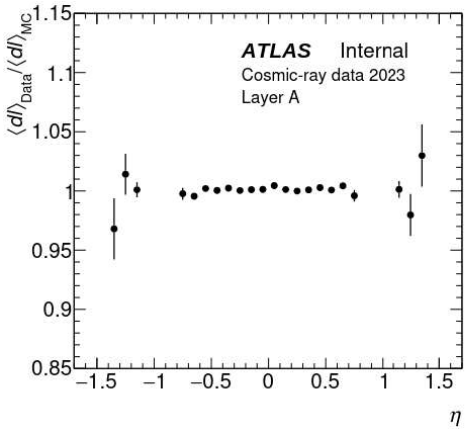

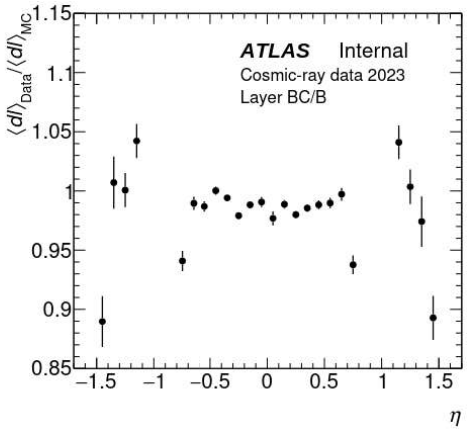

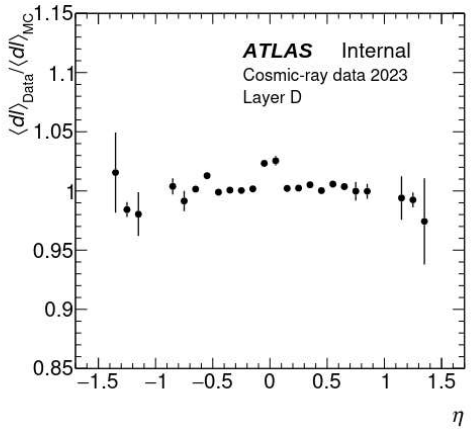

ATL-TILECAL-PUB-2011-001

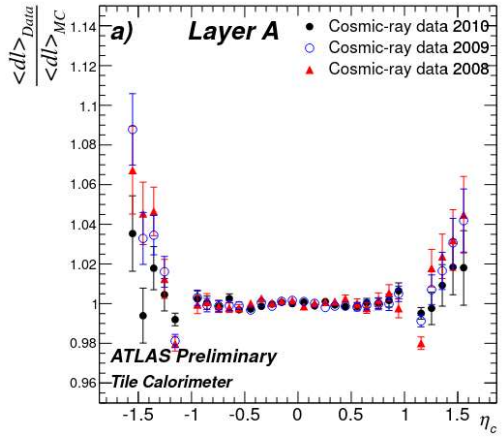

The simulation and the experimental data are consistent within a few percent.

Data/MC of average path length as a function of phi

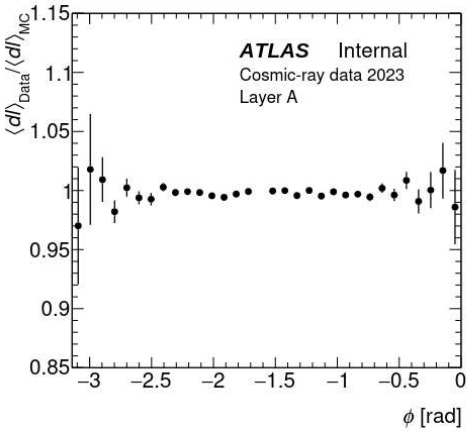

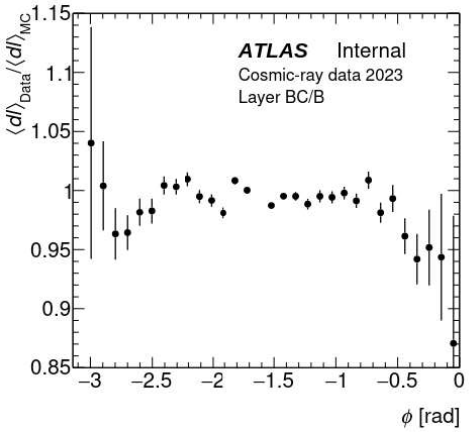

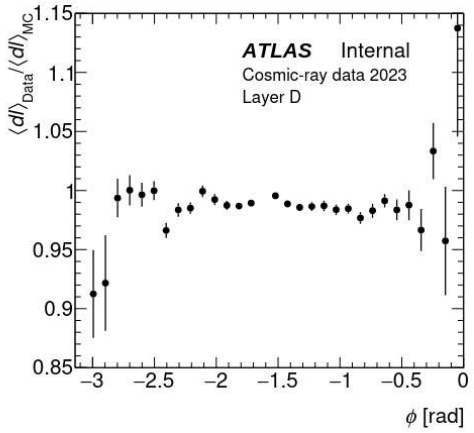

ATL-TILECAL-PUB-2011-001

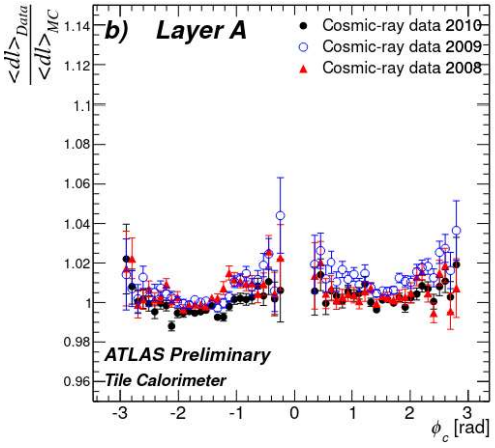

The simulation and the experimental data are consistent within a few percent.

Response dependence on the momentum

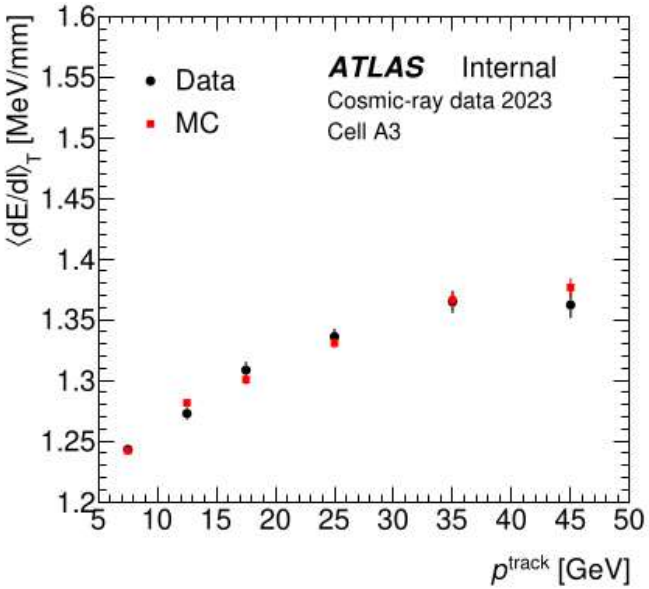

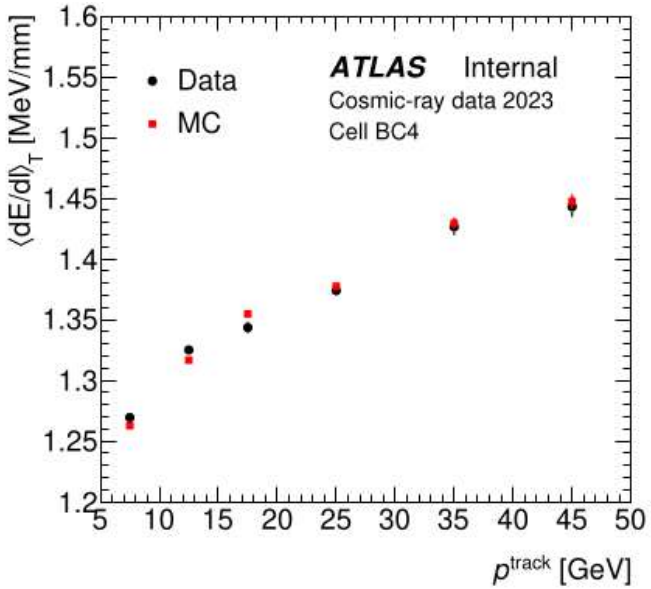

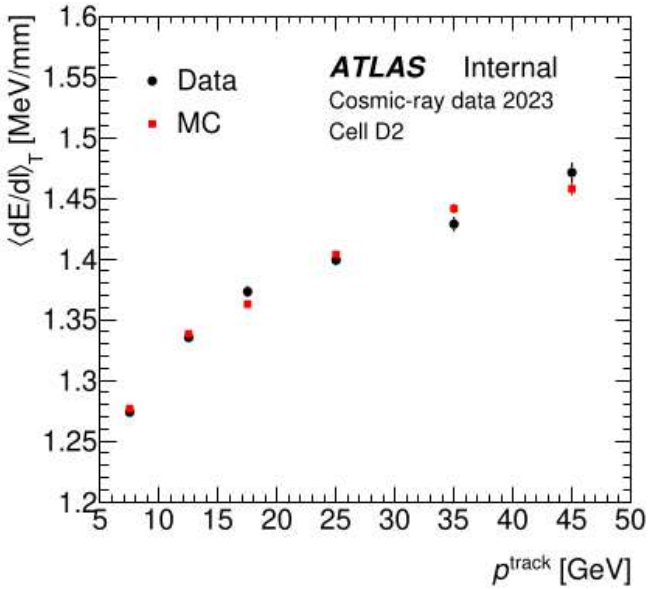

The MC accurately reproduces the response dependence on the momentum observed in the data

Data/MC of average momentum as a function of eta

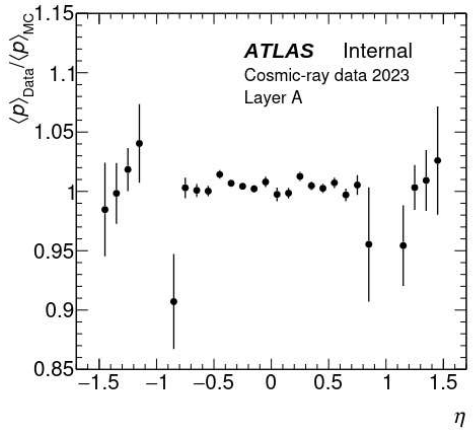

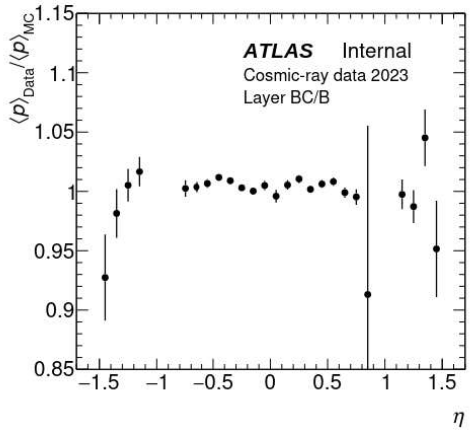

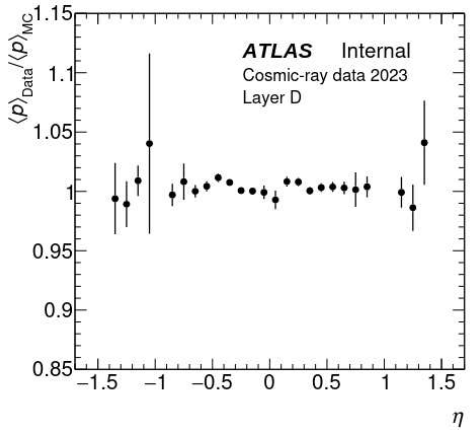

ATL-TILECAL-PUB-2011-001

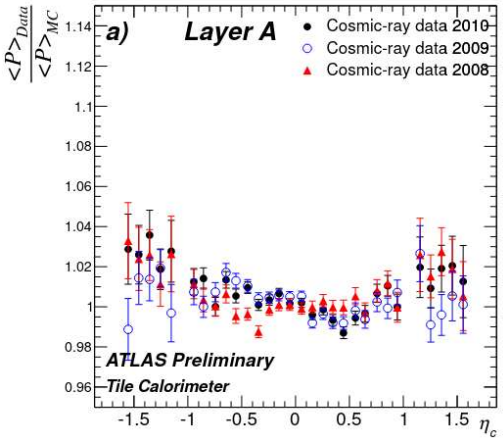

The simulation and the experimental data are consistent within a few percent.

Data/MC of average momentum as a function of phi

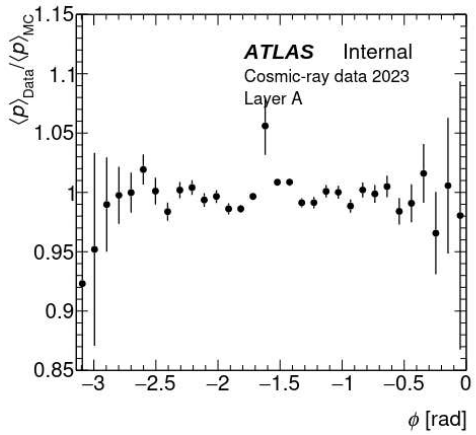

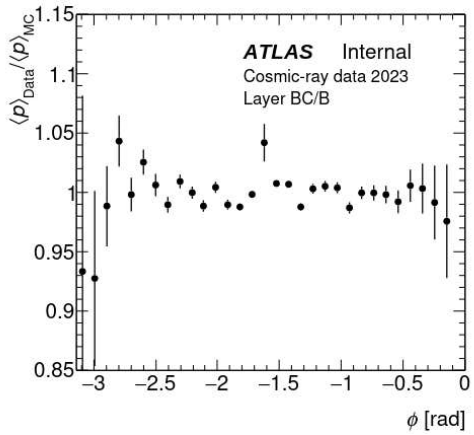

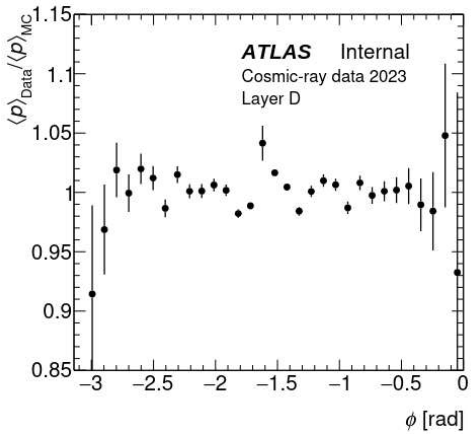

ATL-TILECAL-PUB-2011-001

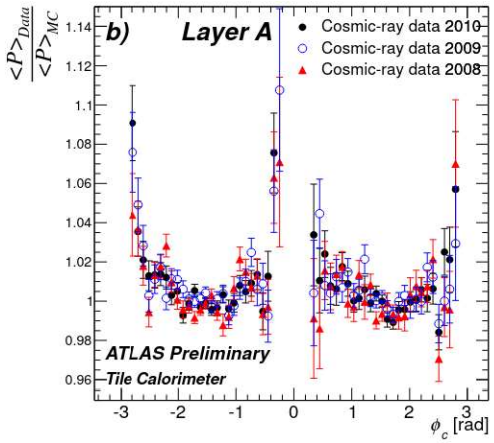

The simulation and the experimental data are consistent within a few percent.

Cell occupancy in eta-phi plane

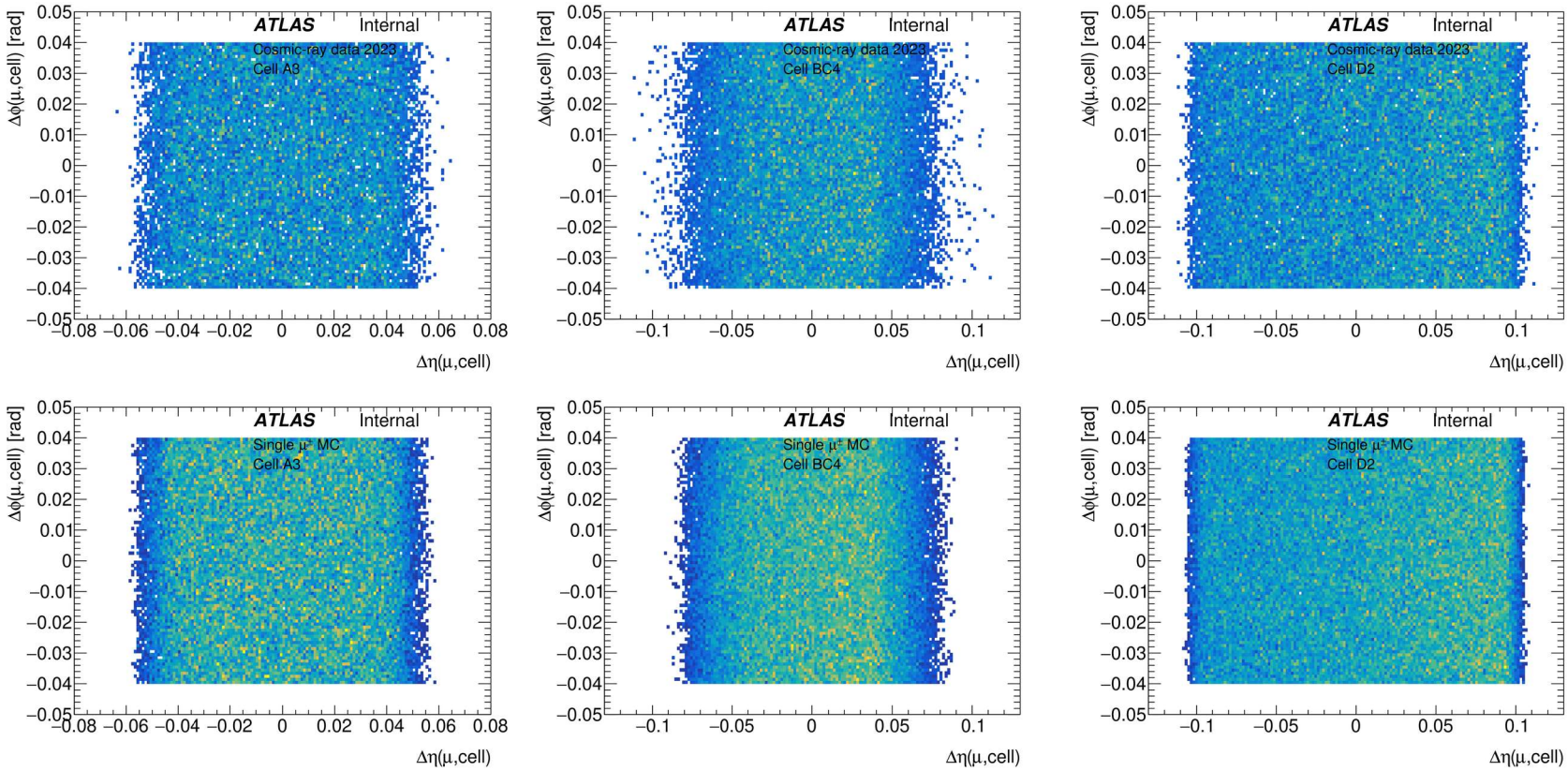

The MC well reproduces the cell occupancy plots observed in the data